Chemical Engineering & Technology Research Article 1

Tony B. Arthur
Nana K. G. Sekyi
Nejat Rahmanian*
Jaan Pu

Process Simulation of Twin-Screw Granulator: Effect of Screw Configuration on Size Distribution

The effect of screw configuration on granule size distribution (GSD) using gPROMS FormulatedProduct (gFP) software to perform optimization, estimation of complex processes, and analyses is evaluated. Twin-screw granulation modeling was used to investigate the contribution of screw configuration and liquid-to-solid (L/S) ratio on GSD. Lactose and Avicel were the granulating materials. Twelve different configurations were investigated under three feed rates as consistent with literature and at various L/S ratios. Results indicate that kneading elements promote the recovery of 100–1000 μm granules while reducing the production of oversized granules. Higher feed rates support the production of fines and agglomerates, while a low feed rate produces 100–1000 μm granules.

Keywords: Agglomerates, Granule size distribution, Kneading elements, Liquid-to-solid ratio, Twin-screw granulator

Received: November 02, 2022; *revised:* January 30, 2023; *accepted:* February 10, 2023

DOI: 10.1002/ceat.202200539

1 Introduction

Granulation is the enlargement process of fine particles adhering to each other to form grain-like agglomerates under a controlled process [1]. This has become a basic pharmaceutical process and is extensively employed in the production of tablets and pellets in the pharmaceutical industry, to improve powder compaction properties and flowability prior to tabletting. Granulation is applied in the pharmaceutical industry for the prevention of product segregation, in promoting powder flowability, enhancing compression of pharmaceutical powders, and preventing dustiness. Granulation is also advantageous for product quality consistency and predictability and process replication [2].

The two main forms of granulation are the wet and dry granulation [3]. The dry granulation is achieved through compressing powder without the use of a liquid medium whiles, the wet granulation makes use of liquid to form bonds that bind the powders together under shear and mechanical stresses to produce granules [4]. The twin-screw granulation technique has in the recent years become one of the major continuous wet-granulation methods that is being employed in the pharmaceutical industries [5].

These recent developments in the use of the technology have spiked interests in the investigation of twin-screw granulation. Thus, several researches have been conducted to examine the process and formulation parameters of the granulation system [6]. Most of these have been about investigating and proposing models based on the formulation, process, equipment, and final product properties [7].

With the advancement in computers, various models and kernels have been proposed for the different stages of the granulation rate process, i.e., nucleation, agglomeration, consolidation, and breakage [8]. It is therefore imperative to use simulation software to implement these models and verify their accuracy by comparing it to experimental data. Although most simulation softwares are very expensive, they prevent material wastage which is an expensive cost to industry and tends to save time. They can also mimic commercial scale-up operations and provide a better avenue in investigating several processes and formulations for onward process optimization if needed [9].

This paper seeks to use simulation software to highlight the effect of screw configuration, L/S ratios, and feed rates on granule size distribution (GSD) by incorporating empirical values proposed by Wang et al. (2021) [10]. The (gPROMS) software is a model builder that has been used to develop the gPROMS FormulatedProduct (gFP) to be able to simulate both steady and dynamic states [11]. Processes that can be defined by a mathematical model can be utilized by gPROMS [12]. In the case of [12–16], the gPROMS and its formulated products have been used to predict experimental results. It is also suitable for

Tony B. Arthur, Nana K. G. Sekyi, Dr. Nejat Rahmanian, Dr. Jaan Pu (n.rahmanian@bradford.ac.uk)
Department of Chemical Engineering, Faculty of Engineering and Informatics, University of Bradford, Bradford, BD7 1DP, UK.

designing experiments and a good estimator of several parameters [12]. These parameters are in the form of equipment parameters, process parameters, and formulation parameters. In this paper, the equipment parameters were considered for analysis where the screw configuration and the formulation parameters were the L/S and the powder feed rate.

2 Design of Simulation

In this paper, a total of 18 different experimental simulations were conducted using the gFP software (see Tab. 1). The simulations are divided into three main forms, with three different granulating formulations. The first group of simulations is labeled experiment "EXP" with a feed rate of the lactose and Avicel being 9 kg h^{-1} and 3 kg h^{-1}, respectively. The second group of simulations is labeled "RUN" and had a feed rate of 7 kg h^{-1} and 1 kg h^{-1}, also of lactose and Avicel blend, respectively. The third group of simulation is labeled "SET" with a feed rate of 8 kg h^{-1} and 2 kg h^{-1} of lactose and Avicel, respectively. The liquid-to-solid ratios (L/S) were 0.1, 0.08, and 0.05 for EXP, RUN, and SET, respectively. Six different screw configurations were simulated in each set of simulation. The screw configuration and arrangements are set out in Tab. 1. These screw configurations as used in this work are with reference and knowledge from already carried-out works [6, 10, 17–19]. All other operating parameters and screw configurations were maintained for all setups.

For this simulation, the granules were not milled or dried. The granules were screened through seven series of sieves (100, 200, 400, 500, 700, 800, and 1000 µm) for the first setup and 12 series of sieves (75, 150, 300, 500, 700, 800, 1000, 1400, 1800, 2200, 2600, and 3000 µm) [20] for the second setup. The evaluation of GSD by the impact of the screw configurations was simulated by employing the two main types of screw elements, i.e., conveying which is labeled "C" and kneading element which is labeled "K" in the description of screw configuration and in the discussions.

2.1 Materials and Methodologies

gPROMS FormulatedProduct (gFP) software was used to simulate the effect of screw configuration on the final granulated product. Lactose and Avicel powders, and distilled water for the granulation simulation were acquired from the gFP material library. The lactose powder had a particle size distribution (PSD) of 15.1, 23.9, and 37.8 µm representing the 25th, 50th, and 75th percentile, respectively, while Avicel had a PSD of 32.7, 76.9, and 143.13 µm also representing the 25th, 50th, and 75th percentile, respectively.

Table 1. Design of simulations, screw configurations for the three different simulations set.

Simulation groups	Labels	L/S	Screw configuration C = conveying, K = kneading [mm]
One	Exp1	0.1	C = 200, K = 20, C = 250, K = 10, C = 160
	Exp3		C = 230, C = 200, K = 30, C = 180
	Exp4		C = 200, K = 20, C = 180, K = 20, C = 100, K = 20, C = 100
	Exp5		C = 200, K = 20, C = 200, K = 20, C = 150, K = 20, K = 30
	Exp6		C = 200, K = 20, K = 30, K = 20, K = 20, C = 200, C = 150
	Exp7		C = 180, C = 110, C = 100, K = 20, C = 100, K = 30, C = 100
Two	Run 1	0.08	C = 200, K = 20, C = 250, K = 10, C = 160
	Run 2		C = 230, C = 200, K = 30, C = 180
	Run 3		C = 200, K = 20, C = 180, K = 20, C = 100, K = 20, C = 100
	Run 4		C = 200, K = 20, C = 200, K = 20, C = 150, K = 20, K = 30
	Run 5		C = 200, K = 20, K = 30, K = 20, K = 20, C = 200, C = 150
	Run 6		C = 180, C = 110, C = 100, K = 20, C = 100, K = 30, C = 100
Three	Set 1	0.05	C = 200, C = 100, C = 160, C = 180
	Set 2		C = 300, C = 300, K = 20, K = 20
	Set 3		C = 100, C = 160, K = 20, C = 120, C = 100, C = 100
	Set 4		C = 200, K = 20, C = 220, K = 20, C = 160, K = 20
	Set 5		C = 300, K = 20, K = 20, K = 20, C = 260, K = 20
	Set 6		K = 20, C = 200, K = 20, C = 180, K = 20, C = 160, K = 20

2.2 Structural Design of the Twin-Screw

The granulator barrel was made up of two inlet ports, one inlet port for the introduction of the powder material and the second port for liquid addition. There was also the outlet stream where the final granules exit the process. The screw length used was 240 mm and the diameter was 20 mm. A sieve analyzer collected the granules into different size distributions. In Tab. 1 investigates the effect of kneading which is an energy-intense element compared to the conveying element on the granule size distribution. Various screw configuration were undertaken under the three different set of simulations. Fig. 1 shows the flowsheet of the simulation in gFP environment.

2.3 Simulation Models

The breakage model used in this research was proposed by Austin et al. [21], and Hounslow (2001) uniform distribution function was applied [21]. In this paper, breakage was assumed to be taking place at the kneading sections along the screws length, thus, the model of Austin et al. [21], which uses the ball sizes to break a particle of any size, is applied. The Austin et al. [21] specific rate of breakage of particles (S_i)[1)] is given by Eq. (1):

$$S_i = \psi X_i Q(z) \tag{1}$$

where ψ is a descriptive constant that has been defined by Eq. (2), X_i is the particle size, α is a constant with a reference value of 0.65 [21], and $Q(z)$ is the Gaussian probability function used in fitting the values for:

$$X_i\psi = \frac{k_2}{d^{1.5}} \tag{2}$$

The constant k_2 in Eq. (2) is expressed as a function of the mill diameter as $k_2 \propto D^{0.6}$. Thus, the descriptive constant α can be determined by substituting the value of D which is the mill diameter and d being the size of the kneading element. The mill diameter in this simulation is the screw diameter.

For layering, the exponential decay formula was applied where the final amount (y) is expressed as:

$$y = ab^{\mathrm{t}} \tag{3}$$

A rate process [22] has given it as:

$$\frac{\mathrm{d}y}{\mathrm{d}x} = ab^{\mathrm{t}} \tag{4}$$

where a is the initial particle size, b is the decaying factor, and t is the time interval. The decaying factor (b = 0.003) was applied in this simulation. Values above or below 0.003 for the decaying factor over- or underpredicted the results for the simulation and occasionally ran the simulation into error. This formula was chosen for a simplistic understanding of the coalescence process.

The layering mechanism is essential concerning granule size as it is one of the most predominant rate process in wet granulation processes [23]. The granule growth rate (G) which is a consolidation/coalescence rate processes is given by Eq. (5) [8]:

$$G = \frac{G_{\mathrm{m}} M_{\mathrm{powder}}}{kM_{\mathrm{granulate}} + M_{\mathrm{powder}}} \exp\left[-(x_w - x_{wc})^2\right] \tag{5}$$

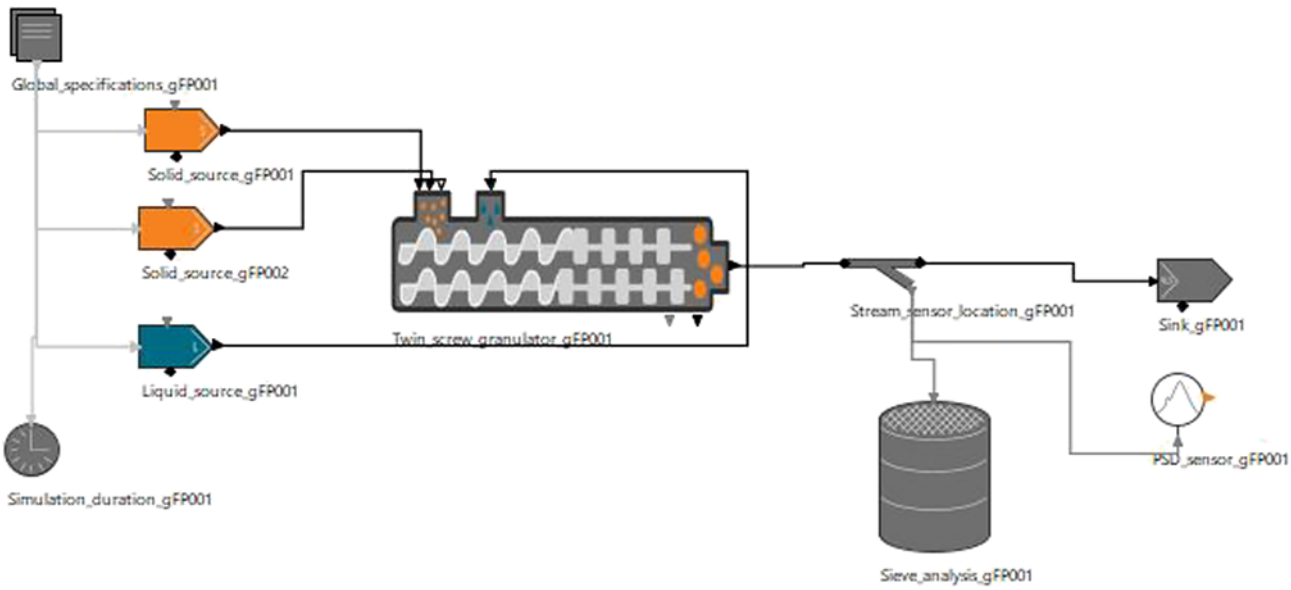

Figure 1. Flowsheet of the process made in gFP software.

1) List of symbols at the end of the paper.

where G_m is the maximum rate of growth, $M_{granulate}$ is the individual mass of granulate, M_{powder} is the mass of unagglomerated powder particles, x_w and x_{wc} are the moisture content of the binder and the critical moisture content, respectively, while k and a are the fitting parameters. The fitting parameters used in this paper were $k = 0.2$ and $\varepsilon = 10$, while G_m was 25 µm s^{-1}. These are reference values from [10].

The population balance model (PBM) is employed to solve the models in Eqs. (1), (3), (4), and (5) in their numerical forms. The PBM is a form of a physical-based modeling which tracks the particle metamorphoses through the granulation mechanism. The PBM in it one- or multidimensional form has been used to predict the gradual changes of granule properties such as granule size distribution, moisture content, density, and porosity [24]. The general equation for representing the PBM is shown in Eq. (6), and Eq. (7) is a general representation of a superstructure of PBM.

$$\delta n/\delta t + \nabla.(vn) - B + D = 0 \tag{6}$$

where v is the particle velocity, n is the number of density particles, and B and D are the particles birth rate and death rate, respectively.

$$\frac{\partial}{\partial t}n(s,l,g,t) + \frac{\partial}{\partial s}\left[n(s,l,g,t)\frac{ds}{dt}\right] + \frac{\partial}{\partial l}\left[n(s,l,g,t)\frac{dl}{dt}\right] + \frac{\partial}{\partial g}\left[n(s,l,g,t)\frac{dg}{dt}\right] = B_{growth}(s,l,g,t) + B_{lay}(s,l,g,t) + B_{break}(s,l,g,t) - D_{break}(s,l,g,t) \tag{7}$$

The vector denoting the solid particles, liquid, and the volume of gas of granule is (s, l, g), and these parameters' granule population density over time is represented as n(s, l, g, t). The three terms on the left-hand side of the equation in the form of partial differential are expressions for change of state due to layering, addition of liquid, and consolidation of gas, respectively. The nucleation and layering net rates are denoted by the first two terms on the right side of the equation as B_{growth} (s, l, g, t) and B_{lay} (s, l, g, t), respectively. Whiles the last two terms represents the birth and death rates due to breakage [25].

2.4 Granule Characterization

For GSD determination, the following sieve ranges were used: 100, 200, 400, 500, 700, 800, and 1000 µm for simulation group 1 with results labeled as "Exp"; 75, 150, 300, 500, 700, 800, 1000, 1400, 1800, 2200, 2600, and 3000 µm in the case of simulation group 2 with accompanying results as "RUN"; and 50, 75, 150. 250, 350, 500, 650, 800, 1000, 1200, 1800, 2600, 4000 µm [19] for simulation group 3 and the results as "SET" as earlier outlined. The difference in choice of sieve sizes is only for granule size detailing each conducted simulation. Nonetheless, the size range of focus is 100–1000 µm regardless of choice of sieves used. The quantity of granules left on each sieve was expressed as a mass fraction (kg kg^{-1}), with the focus range of 100–1000 µm considered for further investigation per author specific interest in cored granule potential usually within this range [26]. The mass fractions of each simulation were calculated. and the resulting GSD compared for discussion based on screw setup and L/S.

3 Results and Discussion

The effect of having more mixing action by kneading elements as compared to the less mixing action by conveying elements in various zones of the screw design has been simulated. Fig. 2 is a GSD of mass fraction per sieve aperture for each of the six simulations under simulation group 1 and with the labels "Exp" 1, 3, 4, 5, 6, and 7. It could be observed that there was a largely small mass fraction of under-fines and a correspondingly high oversized granule fraction which is due to high L/S ratio used. Comparing the mass fraction of oversized granules across all three simulations, the general observation is that the highest L/S ratio of 0.1 yields very high mass fractions of granules above 1000 µm irrespective of the screw configurations [10, 27]. Hence, the overproduction of agglomerates with increased nucleation and growth rates within the system with most of the particles in the setup is bonding easily with each other [19, 28, 29].

From Fig. 2, it is observed that the setups with the least mass fraction of oversized granules above 1000 µm are Exp5, Exp6, and Exp4 in order of increasing mass fraction. These same setups are also seen to promote the formation of granules within

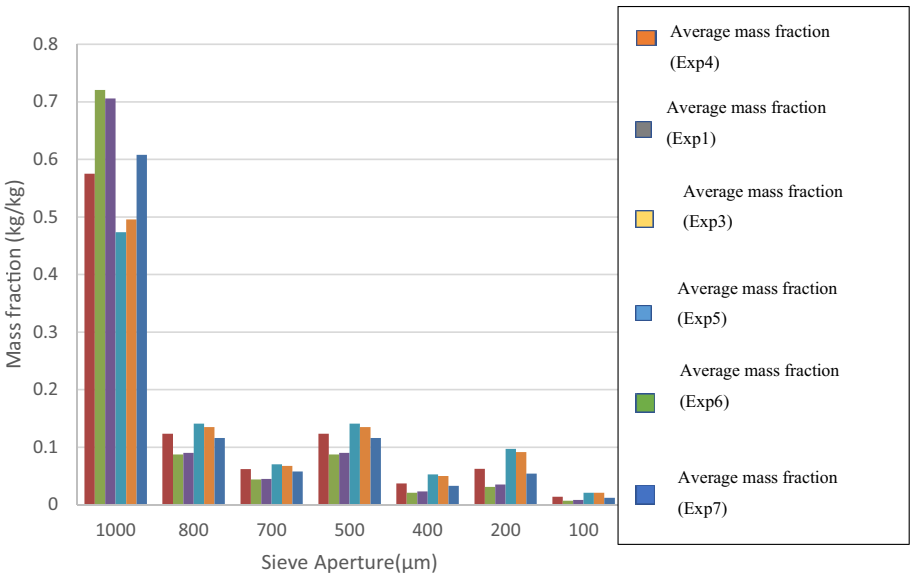

Figure 2. Chart of mass fraction for each screw configuration in the first set of simulations labeled "Exp".

the size range 100–1000 µm but in a reverse order of Exp4, Exp6, and Exp5, respectively, in order of increased granule sizes 100–1000 µm. The most likely explanation for this is a combination of the individual screw arrangements within these experimental setups and, as well, the L/S ratio applied. While Exp6 has a continuous arrangement of kneading elements (KE) with a total length of 90 mm, Exp5 and Exp4 have combined lengths of 90 and 60 mm, respectively, but with intermittent separations by conveying elements.

Another thing to note is that both Exp6 and Exp4 end with conveying elements (CE) per its screw configuration while that of Exp5 ends with kneading elements. With knowledge of KE facilitating formation of more fines [30] and supported from studies by [2], the findings of less oversized granules from Exp5 proves consistent with literature and experimental work. A more recent work by [31] on the impact of kneading and conveying elements within the twin screw granulation process also further justifies the trend observed for Exp5 with low agglomerates and high desired sizes of 100–1000 µm. Since kneading elements promote formation of less sized granules and hinders further agglomeration due to its mechanistic and crushing action [31], it is expected that any setup ending in KE will result in less agglomeration as in Exp5. Again, with CE ending the configurations of Exp6 and Exp4, the tendency of these elements to facilitate more granule growth is confirmed by these simulations as also experimentally proven in [31]. Therefore, though the same high L/S ratio applies to all these varying screw setups, the positioning of the kneading and conveying elements further determines the characteristic sizes formed from the granulation process.

Adding to this on CE tending to promote more granule growth compared with KE, the dominant presence of CE within and at the end of the screw configurations for Exp1, Exp3, and Exp7 supports the simulated results of higher mass fractions of oversized granules in these setups than those discussed earlier (Exp4, Exp5, and Exp6). The effect of CE overshadows the contribution of the KE of total lengths 30 mm (Exp1 and Exp3) and 50 mm for Exp7, respectively. Again, all three setups end in lengthy CE towards the exit of the extruder with the least being 100 mm in the case of Exp7. The order of increasing oversized granules for these three setups is Exp7, Exp3, and Exp1 with Exp1 recording over 60 % oversized granules formed with that of Exp3 and Exp1 being above 70 %.

The production of granules under 1000 µm for screw configurations with a higher number and length of KE suggests intense breakage causing granules to further reduce from already agglomerate sizes which is primarily facilitated by the high L/S ratio used. This breakage by the KE in Exp5, Exp6, and Exp4 reduced the percentage of oversized granules compared to Exp1, Exp3, and Exp7. The production of appreciable granules between 100 and 1000 µm are therefore higher in Exp5, Exp6, and Exp4.

The higher percentages of larger granule size recovered in Exp1 and Exp3 are due to the low number of kneading zones present in the system. The kneading elements are responsible for the breakage rate of the granulation process, thus a lower number/size of kneading zones tends to favor the recovery of larger granules.

3.1 Variation of Conveying and Kneading Elements in the Twin-Screw Granulation (TSG) (Simulation Group 2)

The change in material feed rate as well as L/S ratio appeared not to have affected the GSD that much as the mass fractions are fairly the same as evidenced in simulation 1. The reason for this could be that both simulations 1 and 2 have the same screw configuration setups but with individually unique naming (see Tab. 2 and refer to Fig. 4).

Though more sieve sizes have been added to further separate the granules formed into their relative sizes, the same observation and trend as in simulation group 1 is evidenced for simulation group 2. Higher mass fractions of oversized granules are formed from all six runs studied, with Runs 1, 3, 4, and 6 exhibiting the same pattern particularly at larger sieve apertures between 1000–3000 µm. A cumulative sum of the individual mass fractions recorded for the size range 1000–3000 µm shows that the very high percentages of oversized granules as found for simulation group 1 does not differ much in the case of simulation group 2. Rather, and more interestingly, there seems to be higher mass fractions for simulation group 2 than simulation group 1 when oversized granules greater than 1000 µm are considered. The rational for this is likely to be the reduced feed rate, allowing for more binder and powder interaction, hence improved granule growth in size.

The change in L/S ratio for simulation group 2 is just 0.02 which from the results proves insufficient for significant impact in the granule formation process. Thus, though at a reduced L/S of 0.08, it is not significantly lower than 0.1 in simulation group 1 and the facilitation of agglomerate growth is still dominant. The trend in order of more production of desired gran-

Table 2. Experimental screw configuration equivalence in Simulations 1 and 2 showing KE positioning.

Simulation group 1	Simulation group 2	KE length [mm]	KE positioning
Exp1	Run 1	30 (dispersed)	Towards beginning and end
Exp3	Run 2	30 (continuous)	Towards the end
Exp4	Run 3	60 (dispersed)	Towards beginning, within midsection, and towards end
Exp5	Run 4	90 (continuous)	Towards beginning, midway, and towards end
Exp6	Run 5	90 (dispersed)	Midsection
Exp7	Run 6	50 (dispersed)	Within midsection and towards end

ules under 1000 µm, however, differs from that of simulation group 1, with run 5 having the highest mass fraction. Run 5 with the highest number of four consistent/continuous kneading zones and the combined length of 90 mm produced the highest mass fraction of desirable granule sizes under 1000 µm with a recovery of approximately 31 %.

Runs 1, 6, and 4 then contest closely for the next highest mass fraction of desired granule sizes while run 3 tends to yield the least desired granule sizes under simulation group 2 conditions investigated. This again can be explained by the reduced feed rate which ensures better granulation as more of the powder within the extruder gets coated with liquid binder to facilitate growth. In the case of simulation group 1, the high feed rate also meant that some of the material most likely exited the extruder ungranulated and accounted for the increased mass fraction of fines, irrespective of the screw element setups used (refer to raw powder PSD).

In Fig. 3, the bimodal distribution is demonstrated and the formation of lumps are typical and consistent for such L/S ratios [28]. It is important that the impact of formulation and feed rate on GSD is investigated and well understood as the results from using same configurations but at different L/S ratios suggested above. The assumption made for this simulation is that breakages only take place at the kneading section while granule growth happens along the conveying elements. Nonetheless, growth occurs throughout the screw length and with simultaneous breakages during granulation. The number of kneading elements in run 5 is just enough to break the larger agglomerated granules into appropriate granule sizes.

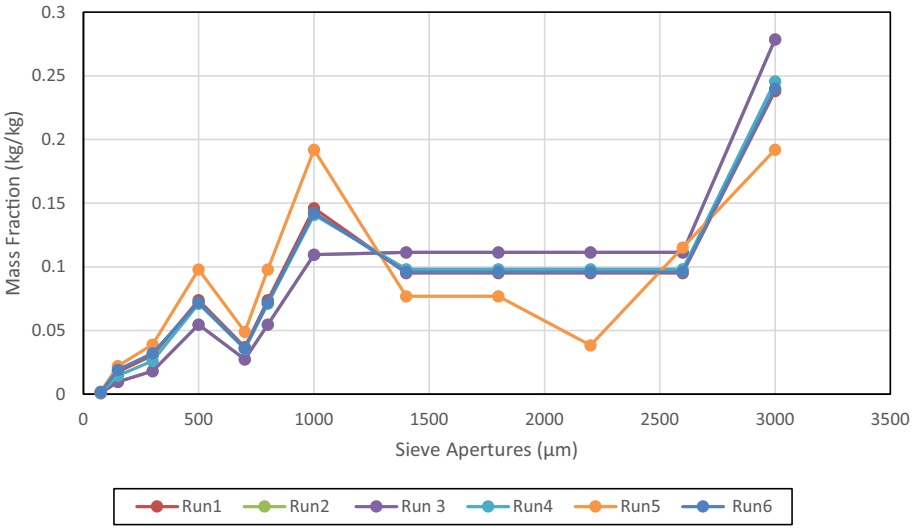

Figure 3. Granule size distribution for each screw configuration in the second set of simulations labeled (setup 2).

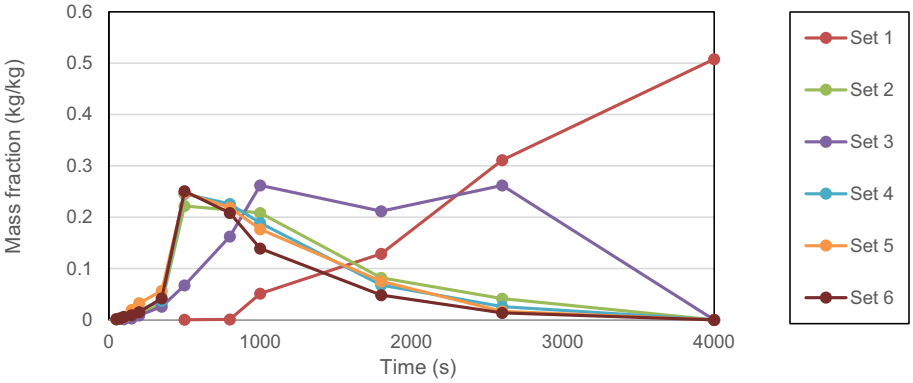

Figure 4. Mass fraction for different screw configuration in the third set of simulations labeled (setup 3).

3.2 Variation of Conveying and Kneading Elements in the TSG (Simulation Group 3)

For simulation group 3 the aim was to analyze the effect of different screw configurations under the formulation parameters of 8 kg h^{-1} feed rate of lactose and 2 kg h^{-1} of Avicel, and the L/S ratio of 0.05. In Fig. 4 the various size distributions for the different screw configurations are illustrated.

To further build on the discussion on the individual contributions of kneading and conveying elements to the formation of granules as detailed in Sect. 3, sets 1, 2, and 3 from simulation group 3 will be further discussed here. Set 1 is an all-conveying arrangement without any KE, set 2 involves a 40 mm length of KE at the very end of the extruder, and finally, set 3 has a 20 mm length of KE midway along the screw length. Observations from Fig. 4 suggest that conveying elements (set 1) favor more granule growth and agglomeration. The agglomerates produced in set 1 are expected due to the lack of a distributive element to aid breakage and consolidation. The lack of KE in set 1 facilitated the ease of oversized granule (> 1000 mm) formation at nearly 100 %.

The presence of the 20 mm length of KE about midway into the full length of the screw configuration in set 3 clearly shows the impact of breakages and crushing by the kneading unit as the continuous rise in the mass fraction of larger granules is impeded in the size range 1000–1800 µm. This however picks up between the range 1800–2600 µm and steeply falls until 4000 µm. The discrepancy in the trend unlike that of set 1 is accounted for by the breaking and crushing action of the kneading elements present. Since the length of KE is short in

comparison with the conveying elements that follow next, facilitation of granule growth resumes over the extended length of CE until material exits the extruder.

For set 2, because of the 40 mm length of KE ending the screw setup towards the end of the extruder, the initial granule growth observed to the size of 350 μm begins to fall steadily to 1000 μm as granules begin to be fed into the kneading zone. On entering the kneading zone, the initially formed agglomerates are consistently crushed and broken down to contribute more to the mass fraction of granules under 1000 μm, further reducing the mass fraction of granules over 1000 μm as clearly evidenced by the trend of granule size over the range of sieve sizes investigated in simulation group 3.

The size distributions in set 4, 5, and 6 follow a similar trend as for set 2 with cumulative recovery rates of appreciable granules above 70 %. Set 2 with two kneading zones at the tail end of the extruder and with a combined length of 40 mm offers the third highest cumulative recovery of appreciable granules, with the order of favored appreciable granule size formation being set 4 > set 5 > set 2 > set 6. Another observation that supports the already established action of the kneading zone is the significant reduction in agglomerates for all sets with screw configurations ending with KE (i.e., sets 2, 4, 5, and 6).

3.3 Effect of Feed Rate and L/S Ratios

Simulations 1, 2, and 3 have feed rates of 12, 8, and 10 kg h^{-1}, respectively, and corresponding L/S ratios of 0.1, 0.08, and 0.05. Comparisons of simulations 1 and 2 suggest that increasing the feed rate for same screw arrangements increases the percentage of fines (< 100–150 mm) and this is regardless of the slightly higher L/S ratio accompanying the increase in feed rate this is consistent with [10]. Therefore, it can be assumed that to compensate for an increase in feed rate and to reduce production of more fines, a significant raise in the L/S ratio must be applied. The higher feed rate in simulation group 3 with completely different screw arrangements from simulations 1 and 2 also suggests the tendency of more fines forming when compared to simulation group 2 which has the least feed rate out of the three.

Although simulation group 1 has higher powder flow rate when compared with simulation group 3, its higher L/S hints at a reduction in the mass fraction of fines produced per the simulated results. This is highly evident when directly compared to results of simulation group 3 which has a lower L/S to that of simulation group 1. It can therefore be said that increasing the L/S to some extent favors the production of appreciable granules as overly larger L/S may lead to overwetting and pasteurizing of the powder. This is consistent with the work described in [32] on the effect of L/S on granule properties where the L/S was found to be directly proportional to the torque and the resistance time. While the oversized granules produced at the low L/S ratio are attributed to the liquid bridges with powder not being enough due to the low amount of granulating liquid, the opposite was for higher L/S. With less L/S ratio in simulation group 2 than for simulation group 1 the percentage of granules recorded for the sieve aperture 1000 μm was reduced.

Few examples include a reduction from 58 % to 11 % for run 3 (i.e., Exp4) and 72 % to 15 % for run 1 (i.e., Exp1), respectively. However, a cumulation of all agglomerates above 1000 μm for both run 3 and 1 suggest higher percentage mass fractions of approximately 84 % and 79 %, respectively. This could indicate that this process needs further analysis for an ideal process optimization to determine an ideal feed rate to use for the L/S ratio of 0.08 or vice versa, the ideal L/S to use in combination with the set feed rate of 8 kg h^{-1}, for which the production of appreciable granules rises while there are decreases in both fines and agglomerates [6].

4 Conclusion

The gFP software from Siemens PSE has been used to mimic actual experimental work, and interpretations of the results obtained were made with considerable justification in literature. The effect of screw configuration on the final granule product has been explored and found to be immense. From the results of the gFP simulation it is concluded that the size distribution for larger granules (agglomerates) decreased drastically with increasing number of kneading elements which also tend to promote the recovery of appreciable granule sizes.

Nonetheless, the positioning of kneading elements within the length of the extruder does have an impact of the GSD. With KEs ending the length of the screw arrangement, less agglomerates are produced. The absence of KE within the screw configuration as in set 1 of simulation 3 depicts the free ease of granule growth facilitated by conveying elements which generally promote forward motion. The general school of thought of crushing and breakage occurring at kneading zones has also been justified from the simulation studies and accompanying results.

The granulation of the formulation at different feed rates of the powder is a major contributing factor to GSD. However, to better understand and optimize these, optimal feed rates and corresponding L/S ratios need to be identified for which appreciable sized granule production is maximized with reductions in fines and agglomerates. Although granulating at different feed rates seems to produce relatively similar GSDs, granulating at higher feed rate tends to produce comparatively higher fractions of fines and oversized granules while granulating at lower feed rates tend to favor the production of high fractions of appreciable granules. It could be concluded that increasing the feed rate raises the production of fines with a higher probability of these being ungranulated feed materials.

The effect and usefulness of the kneading element in twin-screw granulation was established. The impacts of feed rate and L/S on granule size distribution were assessed using the gFP software. This software has been proven capable of simulating the twin-screw granulation process, similar to results from experimental work in the literature.

Acknowledgment

Special gratitude is given to Siemens PSE UK for providing the software resource for this research and to Ghana Scholarship Secretariat for providing the necessary funding.

The authors have declared no conflict of interest.

Symbols used

a	[μm]	initial particle size
b	[–]	decaying constant
d	[μm]	size of screw diameter
D	[μm]	mill diameter
G	[μm s^{-1}]	granule growth rate
G_m	[μm s^{-1}]	maximum rate of growth, individual
K	[–]	fitting parameter
k_2	[–]	constant expressed as a function of the mill diameter as $k_2 \propto D^{0.6}$
$M_{granulate}$	[g]	mass of granulate
M_{powder}	[g]	mass of unagglomerated powder particles
$Q(z)$	[–]	Gaussian probability function
S_i	[h^{-1}]	specific rate of breakage
t	[s]	time
X	[μm]	instantaneous particle size
x_w	[g m^{-3}]	moisture content of binder
x_{wc}	[g m^{-3}]	critical moisture content
Y	[μm]	final particle size

Greek letters

α	[–]	constant with a reference value of 0.65 [21]
ε	[–]	fitting parameter
ψ	[–]	descriptive constant that has been defined by $x_i\psi = \frac{k_2}{d^{1.5}}$

Abbreviations

gFP	gPROMS FormulatedProduct
GSD	granule size distribution
KE	kneading element
L/S	liquid-to-solid
TSG	Twin-Screw granulation

References

[1] L. Kotamarthy, R. Ramachandran, *Powder Technol.* **2021**, *390*, 73–85. DOI: https://doi.org/10.1016/j.powtec.2021.05.071

[2] R. M. Dhenge, R. S. Fyles, J. J. Cartwright, D. G. Doughty, M. J. Hounslow, A. D. Salman, *Chem. Eng. J.* **2010**, *164 (2–3)*, 322–329. DOI: https://doi.org/10.1016/j.cej.2010.05.023

[3] S. Shanmugam, *BioImpacts* **2015**, *5 (1)*, 8.

[4] S. Pohl, P. Kleinebudde, *Int. J. Pharm.* **2020**, *587*, 119660. DOI: https://doi.org/10.1016/j.ijpharm.2020.119660

[5] K. M. Kyttä, S. Lakio, H. Wikström, A. Sulemanji, M. Fransson, J. Ketolainen, P. Tajarobi, *Powder Technol.* **2020**, *376*, 187–198. DOI: https://doi.org/10.1016/j.powtec.2020.08.030

[6] R. M. Dhenge, R. S. Fyles, J. J. Cartwright, D. G. Doughty, M. J. Hounslow, A. D. Salman, *Chem. Eng. J.* **2010**, *164 (2)*, 322–329. DOI: https://doi.org/10.1016/j.cej.2010.05.023

[7] W. H. AlAlaween, B. Khorsheed, M. Mahfouf, G. K. Reynolds, A. D. Salman, *Powder Technol.* **2020**, *364*, 135–144. DOI: https://doi.org/10.1016/j.powtec.2020.01.052

[8] I. T. Cameron, F. Y. Wang, C. D. Immanuel, F. Stepanek, *Chem. Eng. Sci.* **2005**, *60 (14)*, 3723–3750. DOI: https://doi.org/10.1016/j.ces.2005.02.004

[9] T. B. Arthur, J. Chauham, N. Rahmanian, *Chem. Eng. Trans.* **2022**, *95*, 241–246. DOI: https://doi.org/10.3303/CET2295041

[10] L. G. Wang, J. P. Morrissey, D. Barrasso, D. Slade, S. Clifford, G. Reynolds, J. Y. Ooi, J. D. Litster, *Int. J. Pharm.* **2021**, *607*, 120939. DOI: https://doi.org/10.1016/j.ijpharm.2021.120939

[11] *gPROMS FormulatedProducts: Integrated digital design of robust formulated products and their manufacturing processes*, Vol. 2022 (in series), Siemens Process Systems Engineering, London **2022**.

[12] M. Danish, K. B. Ansari, R. A. Aftab, M. Danish, S. Zaidi, Q. T. Trinh, *Environ. Sci. Pollut. Res.*, in press. DOI: https://doi.org/10.1007/s11356-021-13207-y

[13] A. A. Harraz, J. Freeman, K. Wang, N. Mac Dowell, C. N. Markides, *Energy Procedia* **2019**, *158*, 2360–2365.

[14] M. Danish, K. B. Ansari, M. Danish, *Environ. Sci. Pollut. Res.*, **2022**, DOI: https://doi.org/10.1007/s11356-022-20175-4

[15] S. Yoon, S. Galbraith, B. Cha, H. Liu, in *Computer Aided Chemical Engineering*, Vol. 41, Elsevier, Amsterdam **2018**, 121–139.

[16] D. Ntamo, E. Lopez-Montero, J. Mack, C. Omar, M. I. Highett, D. Moss, N. Mitchell, P. Soulatintork, P. Z. Moghadam, M. Zandi, *Digital Chem. Eng.* **2022**, *3*, 100025.

[17] S. V. Lute, R. M. Dhenge, M. J. Hounslow, A. D. Salman, *Chem. Eng. Res. Des.* **2016**, *110*, 43–53. DOI: https://doi.org/10.1016/j.cherd.2016.03.008

[18] R. M. Dhenge, K. Washino, J. J. Cartwright, M. J. Hounslow, A. D. Salman, *Powder Technol.* **2013**, *238*, 77–90. DOI: https://doi.org/10.1016/j.powtec.2012.05.045

[19] J. Vercruysse, A. Burggraeve, M. Fonteyne, P. Cappuyns, U. Delaet, I. Van Assche, T. De Beer, J. P. Remon, C. Vervaet, *Int. J. Pharm.* **2015**, *479 (1)*, 171–180. DOI: https://doi.org/10.1016/j.ijpharm.2014.12.071

[20] J. Vercruysse, D. C. Díaz, E. Peeters, M. Fonteyne, U. Delaet, I. Van Assche, T. De Beer, J. P. Remon, C. Vervaet, *Eur. J. Pharm. Biopharm.* **2012**, *82 (1)*, 205–211.

[21] L. G. Austin, K. Shoji, P. T. Luckie, *Powder Technol.* **1976**, *14 (1)*, 71–79. DOI: https://doi.org/10.1016/0032–5910(76)80009–5

[22] P. C. Kapur, *Chem.Eng. Sci.* **1971**, *26 (7)*, 1093–1099.

[23] K. V. S. Sastry, P. Dontula, C. Hosten, *Powder Technol.* **2003**, *130 (1)*, 231–237. DOI: https://doi.org/10.1016/S0032-5910(02)00271–1

[24] H. Y. Ismail, S. Shirazian, M. Singh, D. Whitaker, A. B. Albadarin, G. M. Walker, *Int. J.Pharm.* **2020**, *576*, 118737.

[25] M. J. Hounslow, M. Oullion, G. K. Reynolds, *Powder Technol.* **2009**, *189 (2)*, 177–189. DOI: https://doi.org/10.1016/j.powtec.2008.04.008

[26] N. Rahmanian, M. Ghadiri, X. Jia, *Powder Technol.* **2011**, *206*, 53–62. https://doi.org/10.1016/j.powtec.2010.07.011
[27] A. Kumar, M. Alakarjula, V. Vanhoorne, M. Toiviainen, F. De Leersnyder, J. Vercruysse, M. Juuti, J. Ketolainen, C. Vervaet, J. P. Remon, K. V. Gernaey, T. De Beer, I. Nopens, *Eur. J. Pharm. Sci.* **2016**, *90*, 25–37. DOI: https://doi.org/10.1016/j.ejps.2015.12.021
[28] A. S. El Hagrasy, J. R. Hennenkamp, M. D. Burke, J. J. Cartwright, J. D. Litster, *Powder Technol.* **2013**, *238*, 108–115. DOI: https://doi.org/10.1016/j.powtec.2012.04.035
[29] W.-D. Tu, A. Ingram, J. Seville, *Chem. Eng. Sci.* **2013**, *87*, 315–326. DOI: https://doi.org/10.1016/j.ces.2012.08.015
[30] M. R. Thompson, J. Sun, *J. Pharm. Sci.* **2010**, *99 (4)*, 2090–2103. DOI: https://doi.org/10.1002/jps.21973
[31] N. K. G. Sekyi, N. Rahmanian, A. L. Kelly, *Chem. Eng. Trans.* **2021**, *86*, 1309–1314. DOI: https://doi.org/10.3303/CET2186219
[32] R. M. Dhenge, J. J. Cartwright, M. J. Hounslow, A. D. Salman, *Powder Technol.* **2012**, *229*, 126–136. DOI: https://doi.org/10.1016/j.powtec.2012.06.019

Research Article: The significant impact of screw configuration on the final granule size distribution was investigated by means of gPROMS FormulatedProduct software to perform optimization, estimation of complex processes, and analyses. Twin-screw granulation modeling was applied to evaluate the contribution of screw configuration and liquid-to-solid ratio on granule size distribution.

Process Simulation of Twin-Screw Granulator: Effect of Screw Configuration on Size Distribution

Tony B. Arthur, Nana K. G. Sekyi, Nejat Rahmanian*, Jaan Pu

Chem. Eng. Technol. **2023**, *46 (XX)*, XXX … XXX

DOI: 10.1002/ceat.202200539